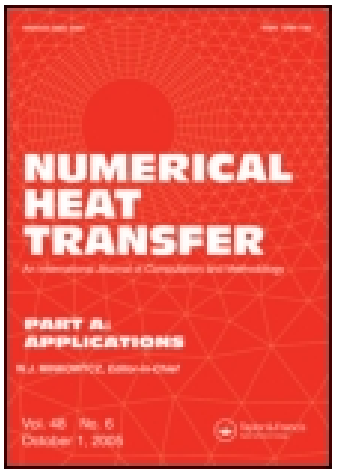

Numerical Heat Transfer, Part A: Applications: An International Journal of Computation and Methodology
Publication details, including instructions for authors and subscription information:
http://www.tandfonline.com/loi/unht20

Predicting Temperature Changes During Cold Water Immersion and Exercise Scenarios: Application of a Tissue-Blood Interactive Whole-Body Model

Anup K. Paul[a], Swarup Zachariah[a], Liang Zhu[b] & Rupak K. Banerjee[a]
[a] Department of Mechanical and Materials Engineering, University of Cincinnati, Cincinnati, Ohio, USA
[b] Department of Mechanical Engineering, University of Maryland, Baltimore, Maryland, USA
Published online: 23 Apr 2015.

To cite this article: Anup K. Paul, Swarup Zachariah, Liang Zhu & Rupak K. Banerjee (2015) Predicting Temperature Changes During Cold Water Immersion and Exercise Scenarios: Application of a Tissue-Blood Interactive Whole-Body Model, Numerical Heat Transfer, Part A: Applications: An International Journal of Computation and Methodology, 68:6, 598-618, DOI: 10.1080/10407782.2014.994417

To link to this article: http://dx.doi.org/10.1080/10407782.2014.994417

Numerical Heat Transfer, Part A, 68: 598–618, 2015

ISSN: 1040-7782 print/1521-0634 online
DOI: 10.1080/10407782.2014.994417

Taylor & Francis
Taylor & Francis Group

PREDICTING TEMPERATURE CHANGES DURING COLD WATER IMMERSION AND EXERCISE SCENARIOS: APPLICATION OF A TISSUE–BLOOD INTERACTIVE WHOLE-BODY MODEL

Anup K. Paul[1], Swarup Zachariah[1], Liang Zhu[2], and Rupak K. Banerjee[1]

[1]*Department of Mechanical and Materials Engineering, University of Cincinnati, Cincinnati, Ohio, USA*

[2]*Department of Mechanical Engineering, University of Maryland, Baltimore, Maryland, USA*

A whole-body model with tissue–blood interaction was simulated to predict (1) cooling during cold water immersion of the human body in water temperatures of 18.5°C, 10°C, and 0°C and (2) heating of the human body at walking intensities of 0.9, 1.2, and 1.8 m/s for 30 min. The transient responses of body and blood temperature were obtained by simultaneously solving Pennes' bioheat and energy balance equations. Predicted survival time at 0°C was around 39–50 min. During exercise with sweating, core body temperature was regulated within 0.25°C of its steady state value of 37.23°C.

1. INTRODUCTION

Evaluating the thermal response of the human body under various scenarios of heat or cold stress is known to be highly challenging. The objective of using the human body model is to compute the steady state and transient responses of the human body under a variety of environmental conditions and physical activities. This can be achieved by realistic modeling of the human thermoregulatory system and its interaction with the surroundings.

Pennes' bioheat equation [1] was developed in 1948 to determine steady state temperature distribution in the human arm, which was modeled as a cylinder. This model incorporated significant physiological details such as variation in metabolic heat generation, blood perfusion, and radial heat conduction. Additionally, heat loss from the surface of the cylinder by convection, radiation, and evaporation was included. In the Pennes' bioheat equation used in this study, blood temperature (T_{blood}) is applied as a steady state initial value at the beginning of the transient

Received 11 September 2014; accepted 1 December 2014.

Anup K. Paul and Swarup Zachariah have contributed equally to this work.

Address correspondence to Rupak K. Banerjee, Department of Mechanical and Materials Engineering, University of Cincinnati, Cincinnati, Ohio, 45221, USA. E-mail: Rupak.Banerjee@uc.edu

Color versions of one or more of the figures in the article can be found online at www.tandfonline.com/unht.

NOMENCLATURE

BSA	body surface area (m^2)
c	specific heat capacity (J/kg°C)
E_{sw}	heat loss due to sweating (W/m^2)
h	overall heat transfer coefficient (W/m^2°C)
k	thermal conductivity (W/m°C)
M_{sh}	volumetric shivering metabolic heat generation rate (W/m^3)
P_{air}	partial pressure of water vapor in ambient air (mmHg)
P_s	vapor pressure of water at skin temperature (mmHg)
P_v	vapor pressure of water in ambient air (mmHg)
q_m	volumetric heat generation rate due to metabolism (W/m^3)
Q_{ext}	external thermal energy added to or removed from the blood (W)
t	time (s)
T	temperature (°C)
T_{air}	ambient air temperature (°C)
T_{blood}	blood temperature (°C)
T_c	core body temperature (°C)
T_s	average skin temperature (°C)
T_t	body tissue temperature (°C)
T_{wt}	perfusion weighted average tissue temperature (°C)
V	volume (m^3)
V_{body}	volume of human body (m^3)
V_{muscle}	volume of muscle (m^3)
V_{organ}	volume of organ (m^3)
$\%RH$	percentage relative humidity of air
ρ	density (kg/m^3)
ω	local volumetric blood perfusion rate per unit volume of tissue (1/s)
ω_{avg}	volumetric average blood perfusion rate per unit volume of tissue (1/s)

Subscripts

air	air
avg	average
blood	blood
body	body
c	core
ext	external
m	metabolism
muscle	muscle
organ	organ
s	skin
sh	shivering
sw	sweating
t	tissue
w	perfusion weighted average

computations. Pennes' bioheat equation can be applied to multiple subdomains of a human body that can be modeled as a combination of cylinders [2]. Computational models developed around the early 1960s began to closely resemble the geometry of the human body and included realistic boundary conditions to simulate different environmental scenarios. A computational model that resembles the human body is generally referred to as a ''whole-body model'' [2].

The earliest whole-body model was developed by Prof. Eugene Wissler's lab. It is a subdomain-based whole-body model that modeled different parts of the human body as 15 cylinders. Pennes' bioheat equation [1] was used to obtain the temperature distribution in each subdomain. Wissler's model included local physiological factors such as variability in blood flow rate and metabolic heat generation. In addition to these factors, heat loss through the respiratory system and sweating was also included. The vascular network of countercurrent arteries and veins was embedded in individual cylindrical subdomains. This allowed for examination of the thermal exchange from tissue regions to the blood, thereby allowing for the computation of transient variations in T_{blood}. It was found that the results from Wissler's model closely approximated experimental data [3], and it was used extensively in the 1980s and 1990s for predicting body temperature and changes in T_{blood}. Since then, different whole-body models were subsequently developed by Smith [4], Fu [5], Fiala

et al. [6], and Salloum et al. [7]. Similar to Wissler's whole-body model, these all modeled a vascular network in their respective whole-body models.

The primary governing equations used in this study were reported by Zhu et al. [8]. Similar to previous whole-body models, that study implemented Pennes' bioheat equation to predict temperature distribution in the human body with the input of arterial blood temperature. The human body was represented by simplified geometrical shapes such as spheres or cylinders. The vascular network shown in previous studies was replaced by an energy balance equation for determining changes in T_{blood} after its circulation throughout the body. This was accomplished by integrating the energy exchange between blood and surrounding tissue from Pennes' source term. The newly developed whole-body model was tested in regard to cooling by intravenously injecting ice-slurry saline into the whole body to counteract fever and lower body/brain temperature after head injury. The results of the study [8] agree well with both simplified energy balance calculations and clinical observations. This model has the potential to be implemented in other situations involving complicated thermoregulatory systems, as well as for changes in dynamic boundary condition surrounding the human body.

The primary computational result obtained from whole-body models is core body temperature (T_c), which is defined as the average temperature of the internal organs in the human body [2]. The human body strives to maintain T_c close to a normothermic value of approximately 37°C [9]. This is made possible, to a large extent, by the circulatory system that helps in blood perfusion redistribution throughout the human body by either increasing or decreasing cardiac output during cold or heat stress conditions. If the thermoregulatory system fails, severe physiological consequences such as organ failure and/or neurological deficiencies are observed [10]. When the human body is immersed in cold water, factors such as increased heat transfer coefficient and low water temperature lead to a decrease in blood perfusion in the superficial skin and muscle layers, thereby resulting in a decrease in skin temperature. Reduced skin temperature over extended periods of water immersion impedes normal cellular functions, which are countered by bodily reactions such as shivering and increase in blood perfusion. On the other hand, during moderate or high-intensity exercise, thermoregulation in the form of increased blood flow to the skin surface counteracts significant increases in cardiac output to keep up with O_2 demands in the exercising muscles. Sweating on the skin surface can also be triggered to lose heat easily to the environment, especially when the surrounding air temperature is high. If the heat generated in the muscle cannot be effectively removed from the skin surface, both T_{blood} and body temperature will increase. It has been reported that marathon runners' body temperature can easily reach 40°C during competitions [11].

In this study, we further developed the theoretical whole-body model [8] to assess tissue–blood thermal interaction in a human body model under cold water immersion and exercise conditions. The objective of this research is to demonstrate the capability of the model to predict T_c, weighted average tissue temperature (T_{wt}), and T_{blood} by implementing the thermal responses of the human body under two extreme environmental and physiological conditions. The flexibility of the model and its potential for use in other thermoregulation situations and medical treatments are also discussed.

2. METHODS

A realistic human body geometry was developed for cold water immersion (Figure 1*A*) and exercise (Figure 1*B*), respectively. The human model consisted of geometrical shapes representing body parts such as limbs, torso, neck, and head. Additionally, a skin layer was added to the model to simulate vasoconstriction effects [3] during cold water immersion. Heat transfer from the body to its surrounding environment was determined using (1) Pennes' bioheat equation to evaluate temperature distribution around the body and (2) an energy balance equation to calculate the change in T_{blood} during a transient heat transfer process. Pennes' equation is defined as

$$\rho_t c_t \frac{dT_t}{dt} = k_t \nabla^2 T_t + q_m + \rho_{blood}\, c_{blood} \omega (T_{blood} - T_t) \tag{1}$$

where ω is the blood perfusion rate, ρ is the density, c is the specific heat, k is the thermal conductivity, and q_m is the volumetric heat generation rate according to metabolism. During cold water immersion or exercise, it is expected that T_{blood} will continuously decrease or increase, respectively. Consequently, an energy balance equation was derived to compute the change in T_{blood}, where the blood within the subdomains of the body is considered as a single lumped system [8]. The governing equation for T_{blood} is written as

$$\rho_{blood}\ c_{blood} V_{blood} \frac{dT_{blood}}{dt} = Q_{ext} - \int_{V_{body}} \int \int \rho_{blood} c_{blood} \omega (T_{blood} - T_t) dV_{body} \tag{2}$$

where V_{blood} is the total volume of the blood in the body. The changes in T_{blood} depend on the heat exchange between the blood and its surrounding tissue after its circulation

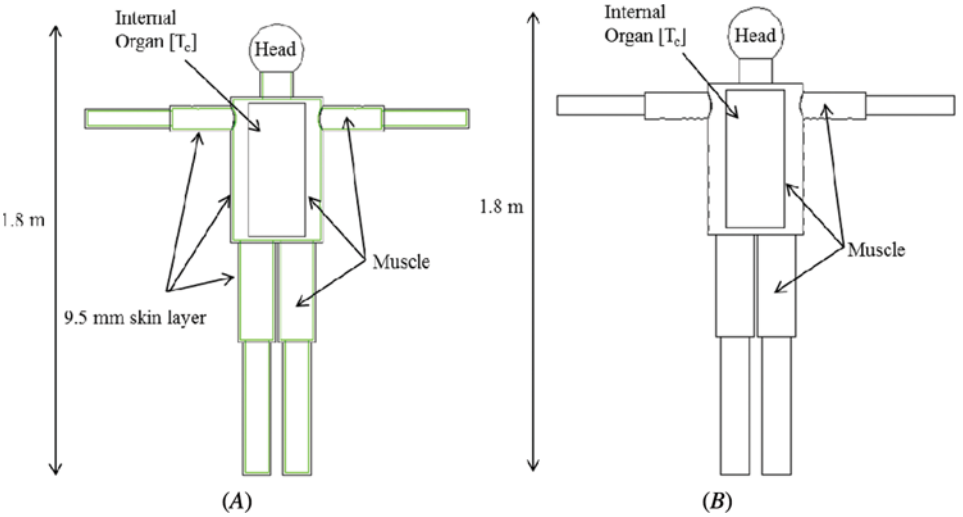

Figure 1. Geometry of a realistic human model for immersion in cold water (*A*) and for exercise scenario (*B*).

in the body. Q_{ext} is the external thermal energy added to or removed from the blood, in units of Watts. However, for cold water immersion or exercise, $Q_{ext} = 0$. The second term on the right-hand side of Eq. (2) represents net heat transfer from the blood to its surrounding tissue, and is calculated by integrating Pennes' perfusion source term in Eq. (1) over the entire body volume (V_{body}). Equation (2) can be further simplified with the introduction of average blood perfusion rate (ω_{avg}) and T_{wt} as shown below:

$$\rho_{blood}\ c_{blood}\ V_{blood}\frac{dT_{blood}}{dt} = -\rho_{blood}\ c_{blood}\ \omega_{avg}(T_{blood} - T_{wt}) \tag{3}$$

where ω_{avg} and T_{wt} are defined as

$$\omega_{avg} = \frac{1}{V_{body}}\int\int\int_{V_{body}} \omega\, dV_{body} \tag{4}$$

$$T_{wt} = \frac{1}{\rho c \omega_{avg}\ V_{body}}\int\int\int_{V_{body}} \rho c \omega T\, dV_{body} \tag{5}$$

As shown in Eq. (3), T_{blood} will decrease when T_{wt} is less than T_{blood} and vice versa. For example, during cold water immersion, a decrease in T_{wt} leads to loss of heat from T_{blood} during its circulation, thereby further lowering T_{blood}. In contrast, during high-intensity exercise, an increase in T_{wt} due to increases in cardiac output and metabolism leads to an elevated level of T_{blood}. Since Eqs. (1) and (2) are coupled, they are solved simultaneously.

Solving a transient heat transfer process requires a prescribed initial condition. In this study, we assume that the initial condition is the normothermic condition achieved (steady state temperature profile for the model), when the body is in thermal equilibrium with the environment. Typically, heat transfer from the human body to its environment is through convection, radiation, and evaporation. In this study, the three possible mechanisms of heat transfer from the body surface are represented by an overall heat transfer coefficient (h) as part of the boundary conditions. During the initial thermal equilibrium, the value of h for an ambient temperature of 25°C is adjusted until T_{wt} is equal to the initial T_{blood} value of 37°C. Consequently, the right-hand side of Eq. (3) is zero, which results in no net energy exchange with the immediate surroundings. This approach is reasonable since an individual can add or remove clothes and turn on or off a fan to feel comfortable, resulting in an adjustable h value.

2.1. Cold Water Immersion Scenarios

Figure 1*A* shows a constructed realistic human body geometry for cold water immersion. A 9.5 mm skin layer was added to the human body model to simulate vasoconstriction effects [3] during cold water immersion. The human model was 1.8 m tall, weighed 80 kg, and had a calculated body surface area (BSA) of 2 m^2 [12]. Similar to the model proposed by Zhu et al. [8], the major computational

Table 1. Physical and physiological parameters for the whole-body thermal model

	Thermal conductivity (W/m °C)	Density (kg/m^3)	Specific heat (J/kg°C)	Blood perfusion (1/s)	Metabolic heat generation (W/m^3)
Muscle	0.5	1,060	3,800	0.0005	553.5
Skin	0.3	1,060	2,802	0.0005*	553.5*
Head	0.5	1,060	3,800	0.00833	9,225
Internal organs	0.5	1,060	3,800	0.001266	1,401.5

*For steady state solution in 25°C air. All physical and physiological properties of muscle, head, and internal organs were obtained from [8]. Skin properties were assumed to be the same as for muscle except for thermal conductivity and specific heat, which were obtained from [13].

subdomains are the muscle, head, internal organs, and skin (Figure 1*A*). The physical and physiological parameters of the muscle, internal organs, skin, and head under ambient conditions are summarized in Table 1 and are similar to those reported by Zhu et al. [8]. The properties of the skin are assumed to be the same as that of the muscle except for thermal conductivity and specific heat capacity [13]. The values of ω_{avg} and V_{body} result in a cardiac output of 0.0054 m^3/min (5.4 L/min), which is consistent with reported values in most medical literature [14]. The volumetric metabolic heat generation rate in each subdomain is assumed to be proportional to that of local blood perfusion rate. The average metabolic rate in the body was approximately 96.85 W, based on a food consumption of 2,000 kcal/day. Total blood volume (V_{blood}) in the body was 0.005 m^3 or 5 L, and the physical properties of blood are assumed to be the same as that of muscle.

Immersion in cold water was simulated by changing the value of h and the water temperature to either 18.5°C, 10°C, or 0°C. The h value for cold water immersion was calculated from energy balance to be 139 W/m^2°C. During cold water immersion, the additional metabolic heat generation rate due to shivering was modeled in the muscles and internal organs using the Tikuisis–Giesbrecht equation [15, 16]. This equation relates the volumetric shivering metabolic heat generation rate (M_{sh}, W/m^3) to changes in average skin temperature (T_s, °C), BSA, volume of muscle (V_{muscle}), volume of organ (V_{organ}), and T_c, as shown below:

$$M_{sh} = \left(32.5(36 - T_c) + 6.6(33 - T_s) - 0.132(33 - T_c)^2\right) \times \left[\frac{BSA}{V_{organ} + V_{muscle}}\right] \quad (6)$$

The shivering metabolic heat generation rate is simply added to the original metabolic heat generation rate in Eq. (1) in the muscle and organ subdomains. Additionally, there was no blood perfusion and heat generation in the skin layer during cold water immersion, thereby simulating vasoconstriction when the skin was exposed to cold water.

2.2. Exercise Scenarios

The realistic human body geometry developed for the exercise scenario (Figure 1*B*) is similar to that for the cold water immersion scenario. However, the

skin layer was not required in this model since vasoconstriction does not occur during exercise. The major computational tissue subdomains (Figure 1*B*) and physical and physiological properties of the muscle, internal organs, and head at resting condition for the exercise model are the same as those in the cold water immersion model (Table 1). Thermal response was calculated for three different exercise intensities of walking on a treadmill at speeds of 0.9, 1.2, or 1.8 m/s. During exercise, about 90% of the heat produced in the body is located in the muscles [17]. Hence, to simulate exercise conditions, metabolic and perfusion rates were modified for muscle only. As shown in Figure 2*A*, the metabolic rate of muscle was allowed to increase linearly from its resting state to a peak metabolic heat generation rate for the respective exercise intensity [18] over 5 min. Local blood perfusion rate was considered to be directly proportional to increases in the metabolic heat generation rate [2], as illustrated in Figure 2*B*.

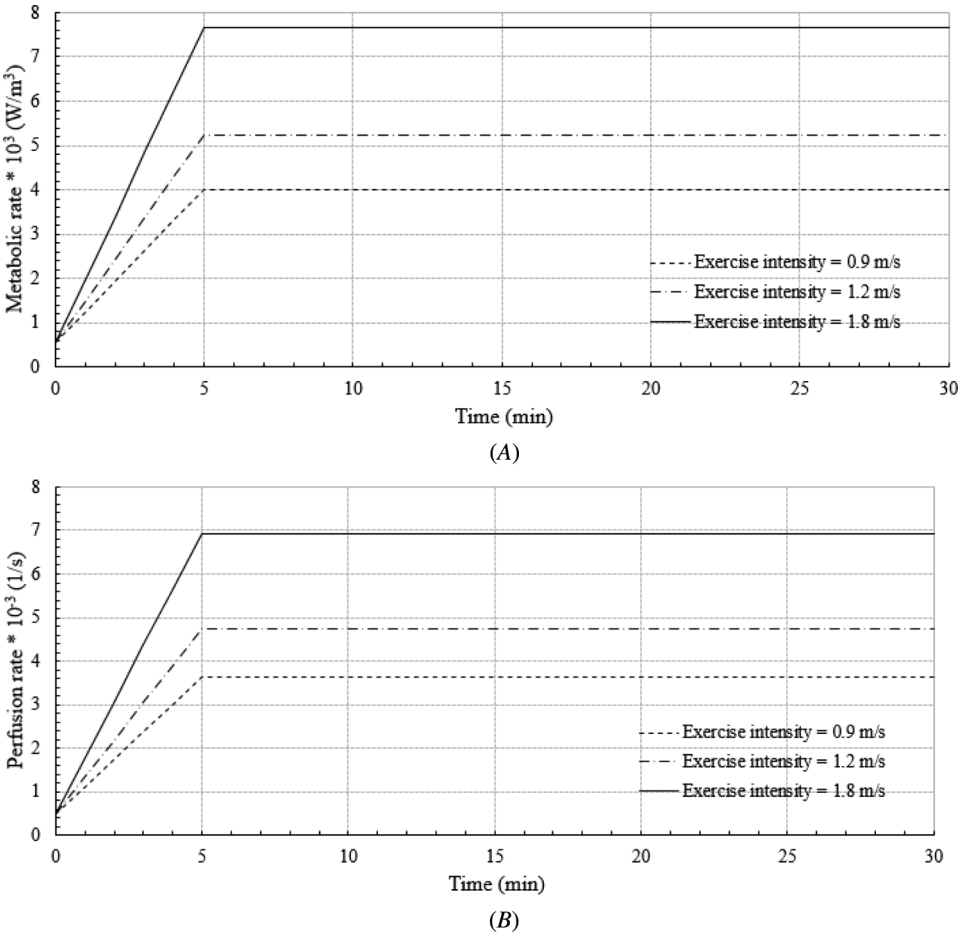

Figure 2. Variation in metabolic rate (*A*) and perfusion rate (*B*) in muscle during exercise.

Thermoregulation during exercise is achieved by increasing blood perfusion rate and inducing sweating. When the increase in local blood perfusion rate is no longer able to successfully regulate body temperature within its acceptable range, the body utilizes sweating as a secondary mechanism to increase removal of heat generated in the exercising muscle. The original boundary condition at the body surface is rewritten as

$$-k_t \left.\frac{\partial T_t}{\partial n}\right|_{at\ surface} = h(T_t - T_{air})|_{at\ surface} + E_{sw} \tag{7}$$

where n is the normal direction of the skin surface. The additional heat loss term in Eq. (7) represents the heat loss due to sweating (E_{sw}, W/m^2). E_{sw} was calculated as a function of the evaporative heat transfer rate (h_e, $W/m^2 \cdot kPa$) and the difference between the vapor pressure of water at skin temperature (P_s, mmHg) and the partial pressure of water vapor in the ambient air (P_{air}, mmHg) [18–21]. The equation for E_{sw} was defined as

$$E_{sw} = 0.1333\left[\frac{\text{kPa}}{\text{mm Hg}}\right] \times h_e(P_s - P_{air}) \tag{8}$$

where P_s and P_{air} were calculated using the following equations:

$$P_s = 1.92\left[\frac{\text{mm Hg}}{^\circ\text{C}}\right] \times T_s - 25.3[\text{mm Hg}] \tag{9}$$

$$P_{air} = P_v \times \%RH \tag{10}$$

In Eq. (10), P_v is the vapor pressure of water at 25°C and $\%RH$ is the percentage relative humidity of air, which was defined as 50%. Parameters were chosen accordingly to incorporate the maximum possible evaporative heat loss in the absence of clothing. Sweating is assumed to begin when T_c exceeds 37.23°C (steady state value of T_c), and thereafter it increases linearly with T_c. The rate of sweating increases to its peak value within a 0.18°C increase in T_c. Figure 3 illustrates the variation in the rate of sweating with T_c during exercise for a fixed skin temperature of 35°C. The maximum possible rate of sweating of 460 W/m^2 (Figure 3) corresponds to a T_c of 37.41°C when the skin temperature is 35°C.

2.3. Numerical Method

The whole-body model was solved using the finite volume solver ANSYS Fluent (v 13.0). Custom functions written in the C programming language were used to include the blood perfusion effect (Eq. (1)) and to solve the energy balance equation (Eq. (2)). Heat generation due to shivering (Eq. (6)), changes in metabolic heat generation rate (Figure 2*A*), local blood perfusion rate (Figure 2*B*), and additional heat loss due to sweating (Eq. (8)) were also included in the whole-body model using custom C program functions. A mesh independence study was performed on the whole-body model developed for the exercise scenario (Figure 1*B*). The finite volume

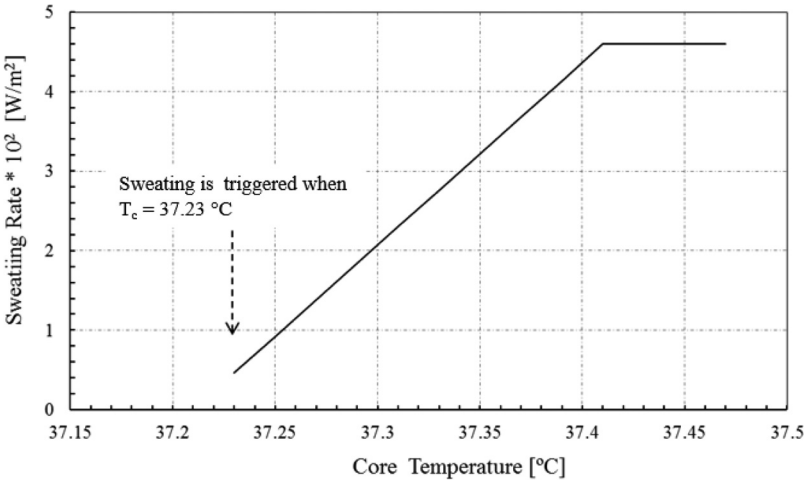

Figure 3. Illustrative example of variation in sweating rate with T_c for a fixed skin temperature of 35°C.

mesh was refined until the change in steady state T_c, T_{wt} and minimum temperature under ambient conditions was below 1%. A total of 60,000 tetrahedral elements were used to model the human geometry for the exercise scenarios. With the addition of the skin layer and using a mesh size similar to that for the exercise model, a total of 118,000 tetrahedral elements were used to model the human geometry for the cold water immersion scenario. A second-order spatial discretization and a first-order implicit transient formulation were employed to solve Pennes' bioheat equation. An implicit scheme was followed in solving the energy balance equation for T_{blood} [8]. Time increments of 1 min were used to solve the transient response of the whole-body model and a convergence criterion of 1e-10 for temperature was achieved within each time increment. The computational time required for the simulation is reasonable (1–2 h).

3. RESULTS

Numerical calculations were performed and analyzed to obtain the spatial and temporal variation in the tissue temperature field in the theoretical whole-body model for the two conditions. The primary result of interest is the temporal variation in T_c during the cold water immersion and exercise scenarios. In addition, the transient trends of T_{blood} and T_{wt} were also determined to show their influence on the temperature field of the body through thermal interactions with tissues.

3.1. Cold Water Immersion Scenario

For immersion in cold water, the steady state normothermic *temperature field* under ambient conditions (25°C air) of the realistic geometry of the human body is presented in Figure 4*A*. The initial value of h for normothermic conditions was determined to be $10\,W/m^{2\circ}C$ for the cold water immersion model. T_t varied between

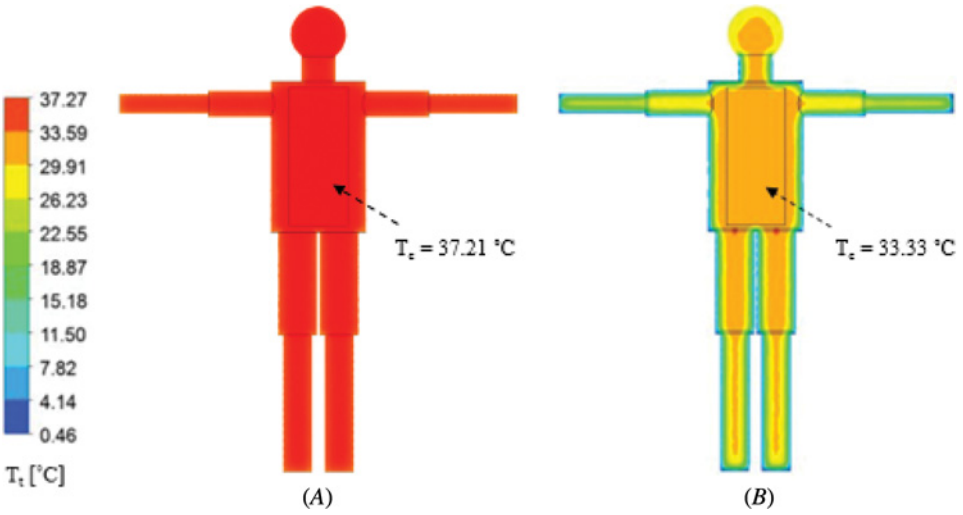

Figure 4. Initial body temperature distribution in 25°C air before immersion in cold water (*A*) and body temperature distribution after 60 min of immersion at 0°C (*B*).

31.55°C and 37.27°C, while T_c was computed as 37.21°C. The steady state temperature field shows almost uniform temperature in the torso and head. However, cooler temperatures were observed in the limbs and skin. As a representative case, Figure 4*B* shows the distribution of T_t after 60 min of immersion in 0°C water. T_t varied between 0.46°C in the limbs and skin and 33.8°C in the torso and head, while T_c was 33.33°C.

3.1.1. Effect of skin layer and shivering. Figure 5 shows the computed change in T_c with or without the skin layer during immersion of the human body in 18.5°C water. Without vasoconstriction in the skin layer, T_c dropped rapidly and reached 33°C within 60 min, which is below the critical T_c for survival. It may be noted that this result includes the heat generation rate due to shivering. Thus, with the skin layer and the effects of vasoconstriction included, the computed value of T_c exhibited a gradual decrease and attained a relatively stable value above the critical temperature of 34.2°C. Moreover, the computed T_c using the computational model with vasoconstriction in the skin layer, as seen in Figure 5, agrees well (variation of 0.5–1.7%) with that calculated using Wissler's detailed whole-body model [3].

The effect of shivering on the computed change in T_c during immersion in 18.5°C water is illustrated in Figure 6*A*. At the end of 80 min of cold water immersion, the simulated T_c with the skin layer but without considering shivering was 4% lower than that computed with shivering. The simulated T_c with shivering shows trends and cooling rates (variation of 0.5–1.7%) similar to those using Wissler's detailed whole-body model [3]. The variation in T_{blood} and T_{wt} during water immersion at 18.5°C, 10°C, and 0°C is illustrated in Figures 6*B* and 6*C*. It is observed that T_{blood} and T_{wt} had the same value (37°C) before water immersion. During the transient computation it will be observed that the temporal value of T_{blood} is somewhat higher (0.02–0.04°C) than T_{wt} at any individual time point, while the trends are

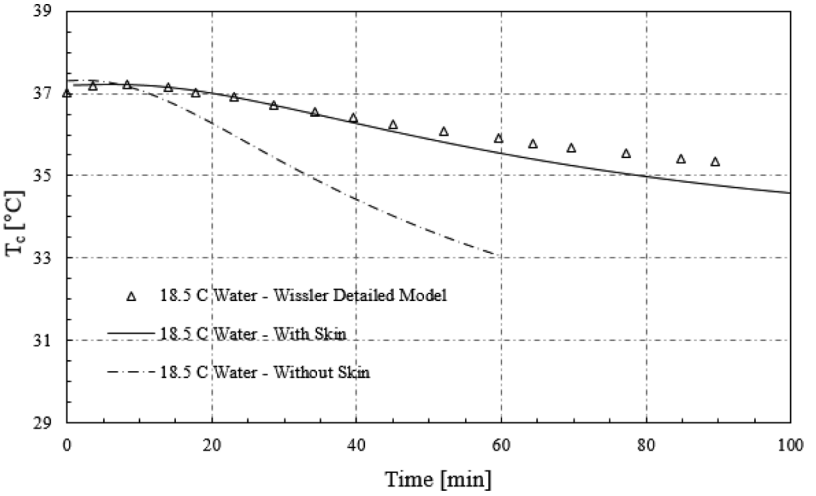

Figure 5. Computed T_c during immersion in 18.5°C water with and without the skin layer included in the human body model.

similar. It may also be noted that T_{wt} and T_{blood} values are lower than the corresponding T_c values.

3.1.2. Variation in T_c. Figure 7 shows the effects of water temperature on the transient variation in T_c and possible survival times predicted by the theoretical whole-body model. It is evident that body temperature decreases faster with colder water. When immersed in water at 18.5°C, the human body is able to establish a relatively stable T_c of 34.5°C after 100 min (Figure 7*A*), whereas it loses heat more rapidly during immersion in water at 10°C or 0°C. After 80 min, T_c dropped to 33.8°C and 32°C during immersion at 10°C and 0°C water temperature, respectively. It is known that the human body enters mild hypothermia at a T_c of 35°C, and the critical T_c for survival typically ranges from 28°C to 34°C [16]. Hence, the survival time for immersion in cold water was determined based on a critical T_c of either 35.21°C (mild hypothermia due to a decrease of 2°C in T_c from its steady state value of 37.21°C) or 34.21°C (a fatal event due to decrease of 3°C in T_c from its steady state value of 37.21°C). The survival times were obtained from the computed change in T_c (Figure 7*A*) and are presented in Figure 7*B*. For immersion in 0°C water, the body enters mild hypothermia after 38 min and death is highly likely after 50 min. An individual can survive in cold water at 10°C for a longer time if he/she is rescued within 70 min. Similarly, for immersion in 18.5°C water, the survival time varies between 72 and 131 min based on a critical temperature of 35.2°C or 34.2°C, respectively.

3.2. Exercise Scenario

The steady state normothermic *temperature field* under ambient conditions (25°C air) of the whole-body model during exercise is shown in Figure 8*A*. The initial overall heat transfer coefficient h for normothermic condition was determined to be 5.1 W/m^2°C. T_c varied between 34.34°C at the finger or toe area and 37.27°C in the

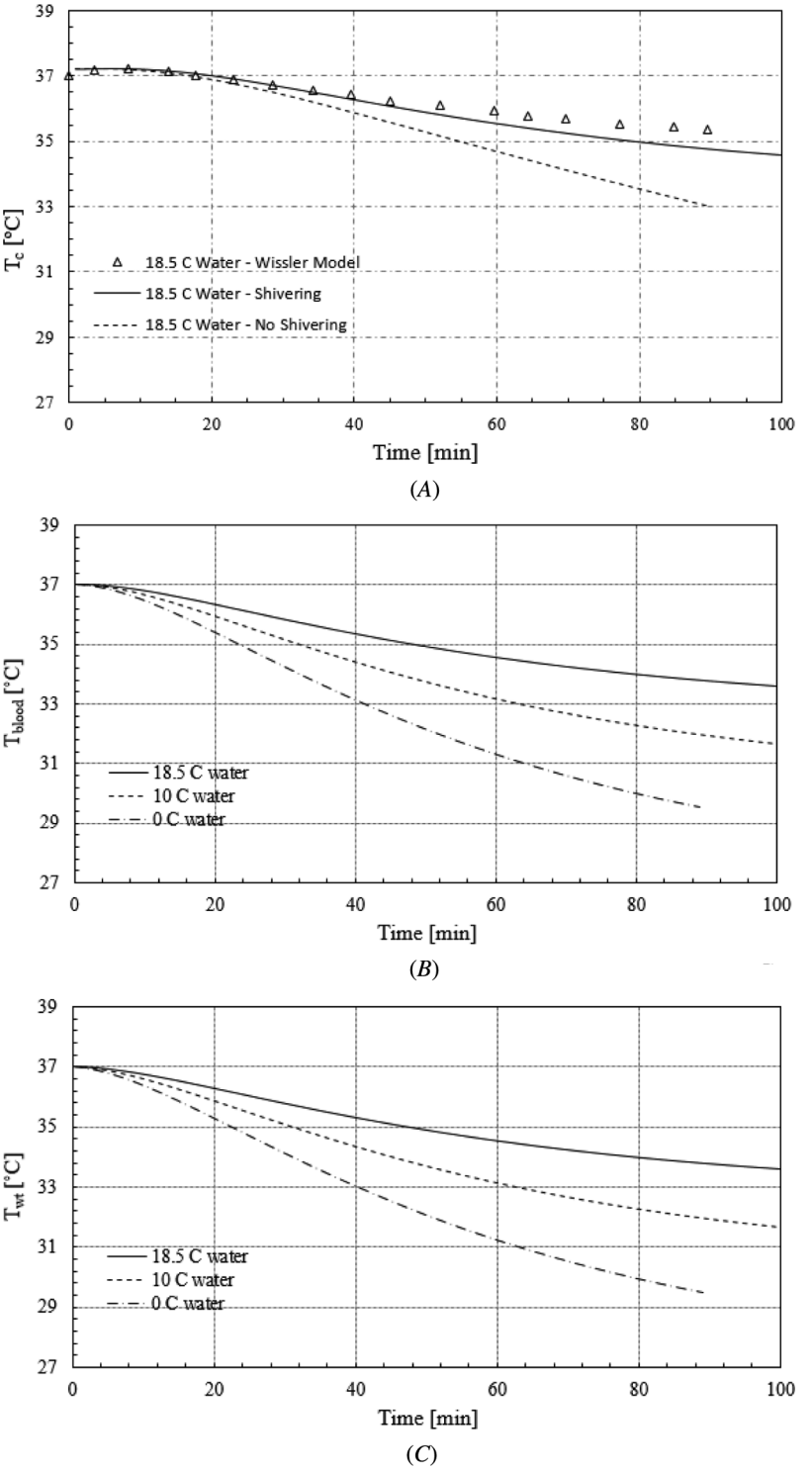

Figure 6. Computed T_c for a realistic human body model during immersion in 18.5°C water with and without shivering (*A*). Variation in T_{blood} (*B*) and T_{wt} (*C*) during cold water immersion.

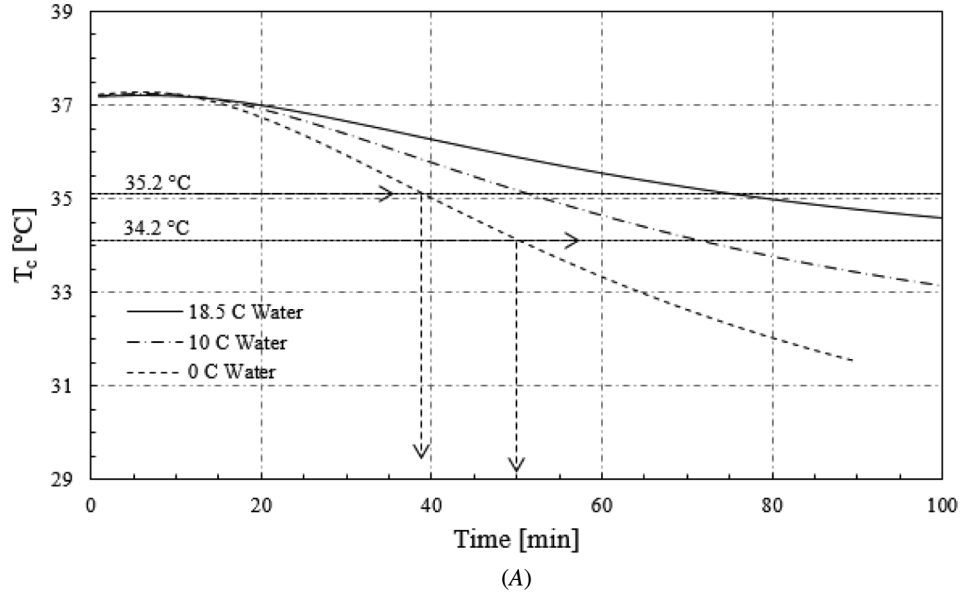

(*A*)

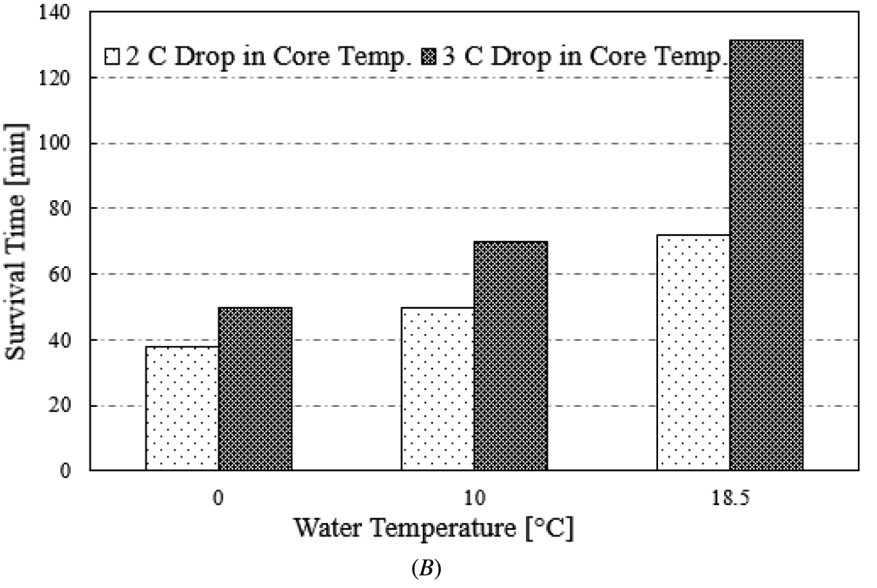

(*B*)

Figure 7. Computed T_c (*A*) and survival times (*B*) for a realistic human body model during immersion in cold water at varying temperature.

brain tissue for the exercise model. It must be noted that the minimum steady state temperature for the exercise model (34.34°C) is higher than that observed for the cold water immersion model (31.55°C). As a representative case, Figure 8*B* shows the temperature field in the human body model after 25 min of exercise at the maximum walking speed of 1.8 m/s with sweating heat loss. T_t varied between

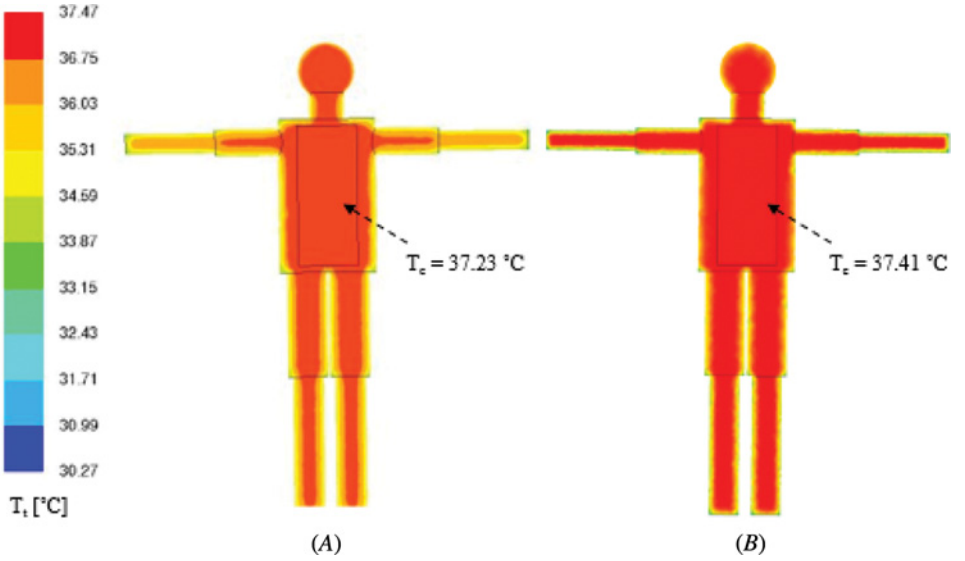

Figure 8. Initial body temperature distribution in 25°C air before exercise (*A*) and body temperature distribution after 25 min of exercise at maximum walking speed of 1.8 m/s (*B*).

30.27°C and 37.47°C, while T_c was 37.41°C, which is relatively higher than its initial value of 37.23°C.

3.2.1. Variation in T_c. Figure 9*A* shows the variation in T_c over time for exercise on a treadmill at different walking intensities without implementing sweating. T_c remained steady for around 2 min as the metabolic and perfusion rates increased in the muscle (Figures 2*A* and 2*B*). Initially a small decrease in T_c was observed after 2 min. This is due to the predominance of the cooling effect caused by the increase in blood perfusion rate (Figure 2*B*) as compared with the heating effect due to elevated metabolism. In the highest-intensity exercise, the downward trend in T_c stopped at 8 min. Subsequently, increase in T_c continued until the completion of the 30 min exercise, with the maxima being 37.43°C, 37.57°C, and 37.83°C for low-, medium-, and high-intensity exercise, respectively.

Figure 9*B1* illustrates how *sweating* at the skin surface helps prevent continuous increase in body temperature. The temperature profile at initial time points in Figure 9*B1* is similar to that in Figure 9*A*. When the walking speed was 1.8 m/s, the onset of sweating was observed when $T_c = 37.23$°C, at $t = 13$ min. The increase in T_c over time, with sweating activated (Figure 9*B1*), for the maximum walking speed of 1.8 m/s is comparatively lower than that observed for the same walking speed with no sweating (Figure 9*A*). However, reduction in T_c was not observed until t = 24 min. The final value of T_c at 30 min was 37.36°C, whereas it would have been 37.83°C if the effect of sweating had not been considered (Figure 9*A*). Similar conclusions can be drawn for the other two walking speeds.

3.2.2. Variation in T_{blood}, T_{wt}, and sweating rate. Figures 9*B2* and 9*B3* depict the transient profiles of T_{blood} and T_{wt} when the sweating was activated. It will

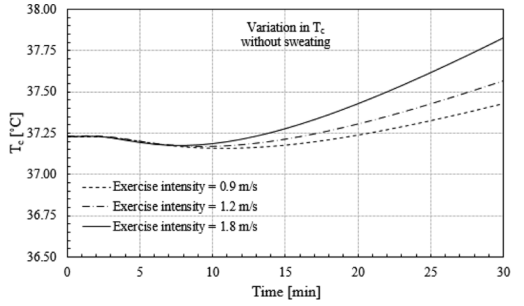

(*A*)

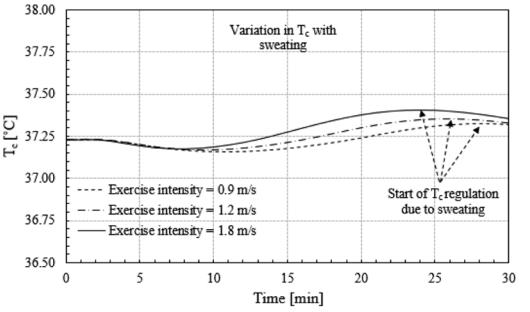

(*B*1)

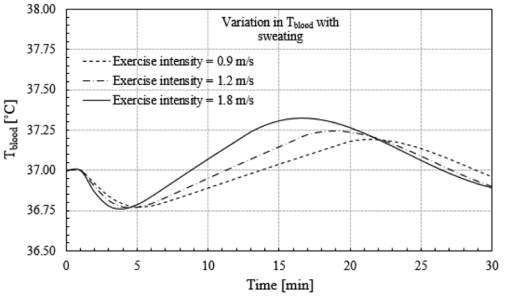

(*B*2)

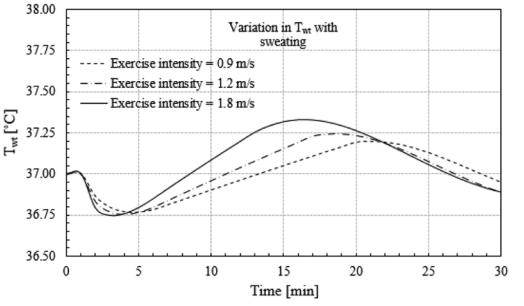

(*B*3)

Figure 9. Variation in T_c without sweating (*A*) and transient variation in T_c (*B1*), T_{blood} (*B2*), and T_{wt} (*B3*) with the inclusion of sweating during exercise.

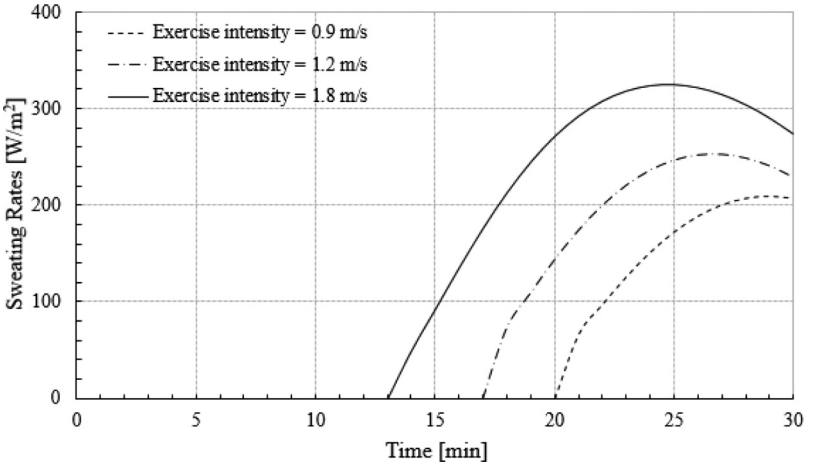

Figure 10. Variation of sweating rate with time during exercise.

be observed that the values for T_{blood} for all three cases are marginally higher than T_{wt} (difference in values is $<0.01°C$). The final values of T_{blood} and T_{wt} at the end of 30 min differ from T_c by around 0.4°C. Figure 10 illustrates the computed variation in the rate of sweating with time. The observed peak rate of sweating, Q_{sw} increased from 210 W/m^2 at a walking speed of 0.9 m/s to 253 W/m^2, and to 325 W/m^2 for speeds of 1.2 and 1.8 m/s, respectively.

4. DISCUSSION

The feasibility of applying the whole-body model [2, 8] to calculate changes in T_c during cold water immersion and exercise conditions has been demonstrated in this study. The whole-body model incorporates variations in metabolic heat generation rates, local blood perfusion rates, shivering, and sweating to compute variations in T_c, T_{blood}, and T_{wt} using transient heat transfer formulations. Cold water immersion and exercise at constant intensity are among the preferred scenarios for assessing human body models [9]. Both ambient temperature and h values can be varied or kept constant, thereby allowing the model to demonstrate its capability to evaluate the influence of variations in environmental conditions on body temperature.

4.1. Variation in Heat Transfer Coefficient (h) Values

The initial normothermic (25°C air) h values for the cold water immersion case and exercise case were iteratively determined to be 10 and 5.1 $W/m^2°C$, respectively. For cold water immersion, the geometry of the human body has an additional 9.5 mm layer of skin. The lower conductivity of skin (Table 1) requires increased convection on the body surface for T_{wt} to attain the value of 37°C, whereas in the exercise scenario, the human body model can achieve a value of 37°C for T_{wt} at a lower h value since the skin layer is not required. It should be noted that the computed initial

normothermic h values are still within the range of acceptable natural convection values in air [21–23].

The differences observed in the *steady state temperature distribution* of the two human body models (Figures 4*A* and 8*A*) are due to the difference in h values. The higher temperature values observed in the head region are due to high metabolic values in the brain tissue. The brain region represents only 2% of a typical body mass but it receives around 11% of cardiac output and accounts for 20% of total oxygen consumption in the body [24, 25]. Similarly, the maximal temperature in the organ zone is also very close to that in the head, due to high metabolic rate and the larger size of the torso. On the other hand, the extremities of the hands and feet have a large ratio of surface area to volume and thus the lowest temperature values are recorded in these regions. The present simulated temperature fields and methodology for computing T_c agree well with those observed in clinical settings. For example, the brain temperature is typically 0.3°C higher than arterial temperature [26]. Further, the rectal location is usually considered as an acceptable site for monitoring T_c [27].

4.2. Influence of Skin, Vasoconstriction, and Shivering

Simulating the variation in T_t during cold water immersion with or without vasoconstriction in the skin layer illustrates the importance of thermoregulation under extreme environmental conditions. Experimental data have shown a similar decrease in T_c over the duration of 60 min for similar environmental conditions [3]. The reduction in blood perfusion through skin due to vasoconstriction in cold environments, and the relatively lower thermal conductivity of the skin, result in high thermal resistance across the skin layer. This causes a smaller decrease in T_c over time. This is reasonable since vasoconstriction slows heat loss from the body, thereby resulting in a slower decrease in tissue temperature (T_t). Another thermoregulatory mechanism is through shivering, which generates heat in the tissue region with reduction in body temperature. A delay in the decrease of T_c over time, under cold stress conditions (Figure 6*A*), is observed as a result of shivering-induced higher metabolic activity within the muscle and internal organs. When the skin layer, shivering, and vasoconstriction are included in the model, a gradual and realistic drop in T_c (Figure 5) was observed. The T_{blood} values of Figure 6*B* are marginally higher as compared with T_{wt} (Figure 6*C*). Additional heat generated due to shivering allows for transfer of heat from the tissue to blood at initial time points. Subsequently, T_{blood} loses its heat to the peripheral tissue regions, which are cooler because of the cold environmental conditions ($h = 139\ W/m^2$). Further, it is of interest to note that T_c values are comparatively high because of the delay in heat exchange from the organ zone to the muscle zone exposed to the cold water. Analysis of the model for different water temperatures demonstrates that with lower water temperature, survival time decreases (Figure 7*B*).

4.3. Variation in Metabolic Rate and Perfusion During Exercise

Under controlled exercise conditions, athletes gradually ramp up their walking speed and then continue at the same intensity till the end of activity. Thus, the muscle metabolic rate was linearly increased over a ramp-up period of 5 min and then held

constant for 25 min at maximum intensity (Figure 2*A*). Since the increase in perfusion is a bodily response to increased metabolic rate [2, 8], blood perfusion was allowed to vary proportionally to metabolic rate (Figure 2*B*). As expected, increases in local blood perfusion values act like a heat sink to counteract the increase in metabolic heat generation. As shown in this analysis, the role of a heat sink is effective initially (Figures 9*A* and 9*B1*). However, blood perfusion is unable to overcome the increased metabolism present during an extended period of exercise and therefore body temperature continues to rise.

4.4. Sweating

The model also evaluates how sweating helps to control increase in body temperature. Sweating during exercise is known to play an important role in thermoregulation of the human body when the surrounding air is relatively dry. When the local blood perfusion rate is unable to regulate T_c within its steady state value of 37.23°C, or if there is a rapid increase in T_c, sweating proves to be a compensating mechanism for cooling the human body. This is because of a significant amount of latent heat released from the skin surface during evaporation of water [28]. As expected, when sweating was not allowed, T_c increases continuously over the entire duration of the exercise (Figure 9*A*) while the rising trend of T_c is reversed to reduce temperature when sweating is allowed to occur (Figure 9*B1*). Despite the occurrence of sweating, the resultant regulation in T_c is observed to begin only after 24–28 min depending on exercise intensity (Figure 9*B1*). The reason for this behavior is twofold: (a) sweating rates are relatively less at lower values of T_c (Figure 3), and (b) there is a time lag between the response of T_c and heat loss from the body surface due to the relatively higher thermal resistance of tissue within the body (Biot number ~4.2).

4.5. Assumptions

The whole-body model implemented in this study can be considered as a simple model as it did not consider detailed geometry of the body and certain physiological factors. For the cold water immersion scenario, reduction in metabolism due to cooling was not considered. Although shivering reduces the cooling rate, its effect can be limited by the possibility of *shivering fatigue* during prolonged exposure of the human body to cold environments [3, 16]. Shivering fatigue was ignored in this study. *Vasoconstriction* is assumed to be instantaneous, while variation in such a phenomenon is reported to be a function of T_c [29]. Literature reports suggest that sweating varies linearly with T_c [20, 30, 31]. Accordingly, linear variation in sweating over a 0.18°C increase in T_c, in conjunction with the trigger value of 37.23°C (steady state T_c value), were assumptions applied in this study (Figure 3). Further, the model assumes uniform sweating over the entire body surface whereas certain regions like the forehead and chest are known to exhibit elevated sweating [23, 32, 33]. Under realistic walking conditions, due to variable air speed [18, 34], *heat transfer coefficient* (h) values vary from one surface area to another of the human body. However, this study considers a uniform h value for the whole-body model. Fat layers under the skin and thermal resistance due to the thickness of clothing materials were not considered in the calculation of heat transfer coefficient. We envision that by (a) adding

additional geometrical details to reflect a realistic human body and (b) accounting for variation in physiological and environmental factors, more accurate prediction of temperature can be obtained. The lumped system described in this study ignores the counter current heat transfer between arteries and veins. It also does not account for spatial variation in T_{blood}. However, one of its advantages is its ability to compute tissue–blood interaction with reasonable accuracy, and without the need for a computationally intensive detailed vasculature network representation of the circulatory system.

The whole-body model evaluated in this study can be used to treat patients who have either hyperthermia or hypothermia. The model can predict changes in T_c and rate of sweating during sporting activities like cycling, running, etc. This would help monitor the patient's/athlete's health. Additional applications for the whole-body model include testing the performance of protective apparel for soldiers, firefighters, deep sea divers, etc. This is expected to ensure effective protection and increased safety.

5. CONCLUSIONS

Variation in T_c under cold water immersion and exercise conditions were calculated in a whole-body model using a tissue–blood interactive equation. It was essential to include the skin layer detail in the geometry for simulating vasoconstriction effects during cold water immersion. The predicted survival time in 0°C was 39–50 min based on a decrease of 2–3°C in T_c. The human body was able to attain a relatively stable T_c of 34°C in a water temperature of 18.5°C. It was shown that the computed drop in T_c during cold water immersion compares well with the results calculated from Wissler's whole-body model. When sweating was allowed for exercise conditions, the computed values of T_c were between 37.41°C and 37.16°C. The relatively small deviation of T_c from its steady state value during exercise was due to the combined effects of change in blood perfusion and sweating-induced evaporation from the skin surface.

DISCLOSURE STATEMENT

The authors report no financial relationships or conflict of interests regarding the content herein.

REFERENCES

1. H. H. Pennes, Analysis of Tissue and Arterial Blood Temperatures in the Resting Human Forearm, *J. Appl. Physiol.*, vol. 1, pp. 93–122, 1948.
2. T. E. Schappeler, Development of an FEA-Based Whole-Body Human Thermal Model for Evaluating Blood Cooling/Warming Techniques, Masters thesis, University of Maryland, Baltimore, Maryland, 2009.
3. E. H. Wissler, Mathematical Simulation of Human Thermal Behavior Using Whole Body Models, *Heat Transfer Med. Biol.*, vol. 1, pp. 325–372, 1985.
4. C. E. Smith, A Transient, Three-Dimensional Model of the Human Thermal System, Ph.D. thesis, Kansas State University, Manhattan, Kansas, 1991.

5. G. Fu, A Transient, Three-Dimensional Mathematical Thermal Model for Clothed Human, Ph.D. thesis, Kansas State University, Manhattan, Kansas, 1995.
6. D. Fiala, K. J. Lomas, and M. Stohrer, A Computer Model of Human Thermoregulation for a Wide Range of Environmental Conditions: The Passive System, *J. Appl. Physiol.*, vol. 87, pp. 1957–1972, 1999.
7. M. Salloum, N. Ghaddar, and K. Ghali, A New Transient Bioheat Model of the Human Body and Its Integration to Clothing Models, *Int. J. Therm. Sci.*, vol. 46, pp. 371–384, 2007.
8. L. Zhu, T. Schappeler, C. Cordero-Tumangday, and A. Rosengart, Thermal Interactions Between Blood and Tissue: Development of a Theoretical Approach in Predicting Body Temperature During Blood Cooling/Rewarming, *Adv. Numer. Heat Transfer*, vol. 3, pp. 197–219, 2009.
9. J. K. Westin, An Improved Thermoregulatory Model for Cooling Garment Applications with Transient Metabolic Rates, Ph.D. thesis, University of Central Florida, Orlando, Florida, 2005.
10. A. Bouchama, Heatstroke: A New Look at an Ancient Disease, *Intensive Care Med.*, vol. 21, pp. 623–625, 1995.
11. M. B. Maron, J. A. Wagner, and S. Horvath, Thermoregulatory Responses During Competitive Marathon Running, *J. Appl. Physiol. Respir. Environ. Exercise Physiol.*, vol. 42, pp. 909–914, 1977.
12. R. D. Mosteller, Simplified Calculation of Body-Surface Area, *N. Engl. J. Med.*, vol. 317, pp. 1098, 1987.
13. R. Skalak and S. Chien, *Handbook of Bioengineering*, McGraw-Hill, New York, 1987.
14. A. Grollman, Physiological Variations in the Cardiac Output of Man, *Am. J. Physiol.*, vol. 89, pp. 366–370, 1929.
15. P. Tikuisis, D. A. Eyolfson, X. Xu, and G. G. Giesbrecht, Shivering Endurance and Fatigue During Cold Water Immersion in Humans, *Eur. J. Appl. Physiol.*, vol. 87, pp. 50–58, 2002.
16. E. H. Wissler, Probability of Survival During Accidental Immersion in Cold Water, *Aviat. Space Environ. Med.*, vol. 74, pp. 47–55, 2003.
17. A. Despopoulos and S. Silbernagl, *Color Atlas of Physiology*, Thieme Stuttgart Inc., New York, 2003.
18. ASHRAE Handbook – Fundamentals, ASHRAE Inc, Atlanta, 2009.
19. E. D. Yildirim and B. Ozerdem, A Numerical Simulation Study for the Human Passive Thermal System, *Energy Build.*, vol. 40, pp. 1117–1123, 2008.
20. D. J. Brake and G. P. Bates, Limiting Metabolic Rate (Thermal Work Limit) as an Index of Thermal Stress, *Appl. Occup. Environ. Hyg.*, vol. 17, pp. 176–186, 2002.
21. G. Havenith, I. Holmér, and K. Parsons, Personal Factors in Thermal Comfort Assessment: Clothing Properties and Metabolic Heat Production, *Energy Build.*, vol. 34, pp. 581–591, 2002.
22. M. Ebrahim Poulad, A. S. Fung, and D. Naylor, Effects of Convective Heat Transfer Coefficient on the Ability of PCM to Reduce Building Energy Demand, 12th Conf. Int. Build. Perform. Simul. Assoc., Sydney, 2011.
23. R. J. de Dear, E. A. Arens, H. P. D. Zhang, and M. Oguro, Convective and Radiative Heat Transfer Coefficients for Individual Human Body Segments, *Int. J. Biometeorol.*, vol. 40, pp. 141–156, 1996.
24. M. E. Raichle, Functional Brain Imaging and Human Brain Function, *J. Neurosci.*, vol. 23, pp. 3959–3962, 2003.
25. D. A. Gusnard and M. E. Raichle, Searching for a Baseline: Functional Imaging and the Resting Human Brain, *Nat. Rev. Neurosci.*, vol. 2, pp. 685–694, 2001.

26. D. A. Nelson and S. A. Nunneley, Brain Temperature and Limits on Transcranial Cooling in Humans: Quantitative Modeling Results, *Eur. J. Appl. Physiol. Occup. Physiol.*, vol. 78, pp. 353–359, 1998.
27. D. S. Moran and L. Mendal, Core Temperature Measurement, *Sports Med.*, vol. 32, pp. 879–885, 2002.
28. S. Nunneley, Water Cooled Garments: A Review, *Space Life Sci.*, vol. 2, pp. 335–360, 1970.
29. E. H. Wissler, Whole-Body Human Thermal Modeling, an Alternative to Immersion in Cold Water and Other Unpleasant Endeavors, *J. Heat Transfer*, vol. 134, pp. 031019, 2012.
30. C. Sussman and B. M. Bates-Jensen, *Wound Care: A Collaborative Practice Manual for Physical Therapists and Nurses*, Aspen Publishers, New York, NY, 1998.
31. D. I. Sessler, Temperature Monitoring and Perioperative Thermoregulation, *Anesthesiology*, vol. 109, pp. 318, 2008.
32. S. N. Cheuvront, M. A. Kolka, B. S. Cadarette, S. J. Montain, and M. N. Sawka, Efficacy of Intermittent, Regional Microclimate Cooling, *J. Appl. Physiol. (1985)*, vol. 94, pp. 1841–1848, May 2003.
33. E. A. Arens and H. Zhang, *The Skin's Role in Human Thermoregulation and Comfort, Thermal and Moisture Transport in Fibrous Materials*, pp. 560–602, Woodhead Publishing Ltd, Cambridge, 2006.
34. F. Wang, Clothing Evaporative Resistance: Its Measurement and Application in Prediction of Heat Strain, Ph.D. thesis, Lund University, Lund, Sweden, 2011.